Conclusions

The goal of the present study was to assess the roles of asymmetric leading-edge flap deflections on delta wings over a wide range of angle of attack, including attached and separated flow regimes. Experimental and computational modeling data were collected for both 80- and 65-deg delta wings with 20% conical flaps.

A significant observation was that both wings exhibited a reversal in control effectiveness at an angle of attack dependent on sweep angle. The reversal behavior may result from the relative strengths of the longitudinal and crossflow effects.

References

[1]Arena, A. S, Jr., and Nelson, R. C., "A Discrete Vortex Model for Predicting Wing Rock of Slender Wings," AIAA Paper 92-4497, Aug. 1992.

[2]Roberts, S. D., and Arena, A. S., Jr., "An Inviscid Model for Evaluating Wing Rock Suppression Methodologies," AIAA Paper 94-0808, Jan. 1994.

[3]Ize, C., and Arena, A. S., Jr., "Spanwise Camber and Quasi-Steady Effects During Wing Rock," AIAA Paper 97-0325, Jan. 1997.

[4]Wentz, W. H., Jr., and Kohlman, D. L., "Vortex Breakdown on Slender Sharp-Edged Wings," *Journal of Aircraft*, Vol. 8, No. 3, 1971, pp. 156–161.

Identifying Aerial Bomb's Aerodynamic Drag Coefficient Curve Using Optimal Dynamic Fitting Method

Yangquan Chen*
National University of Singapore, Singapore 119260, Singapore
Changyun Wen†
Nanyang Technological University, Singapore 639798, Singapore
and
Mingxuan Sun‡
Xi'an Institute of Technology, 710032 Xi'an, People's Republic of China

Introduction

TO increase the bombing accuracy of aerial bombs from aircrafts, the use of the aerial bomb's drag coefficient curve plays a crucial role. There are two ways to obtain such a curve. The first is by wind-tunnel testing. The second is by theoretical numerical prediction. As, when bombing, the mechanism of the interference air flowfield between the aircraft and the aerial bomb is not yet clear at the present time, the drag coefficient curve obtained from either wind-tunnel measurements or theoretical numerical prediction under the free airflow condition cannot be applied directly. The curve reduced from real flight testing data is obviously advantageous in practical applications. Many efforts have been made in identifying aerodynamic properties of real or full-scale flying vehicles from flight-testing data.[1–5] Most existing literature only emphasizes the aerodynamic coefficient extraction by parameter identification. Directly identifying aerial bomb's aerodynamic coefficient curve, especially the Mach history, has not yet been discussed. Also, it has been argued that the time history of the aerodynamic property is not preferred to be extracted directly.[6] In fact, from the intrinsic characteristic of aerodynamics, the aerodynamic property curves (Mach history) are generally invariant in different flight tests if the angle of attack along the trajectory is small, and can be regarded as deterministic control profiles from the control point of view. The aerodynamic property curve identification can then be considered as an optimal tracking control problem (OTCP), where the aerodynamic property curve is the control profile and the flight testing data are the desired trajectories to be optimally tracked. This identified curve is called aerial bomb's optimal fitting drag coefficient curve $C_{df}(M)$. This optimal control problem can be solved by nonlinear programming via a parameterization of the control function,§ but only the time history of the control can be considered. In this Note, the control profile $C_{df}(M)$, rather than $C_{df}(t)$, is directly considered by an optimal dynamic fitting scheme. In the scheme, $C_{df}(M)$ is parameterized by cubic splines with a deficiency number of 2. Thus, the first-order derivative of $C_{df}(M)$ is guaranteed to be continuous. The standard Newton–Raphson iteration is applied. To reduce the computational cost, an idea of quasi-Newton–Raphson iteration is proposed. This can also achieve the second-order convergence that cuts the computing cost by half, even if the first-order gradient alone is used. In addition, the initial system states for flight testing, which may be uncertain or inaccurate, can be easily identified or corrected together with the optimal dynamic fitting procedure. As real flight testing was conducted to obtain the data for aerodynamic curve identification, we believe that the obtained results are rather convincing in applications including the verification and improvement of design objectives, validation of computational aerodynamic property prediction codes, etc.

Problem Formulation

To simplify our discussion, a three-degree-of-freedom point mass ballistic model is used. Suppose at time t, the aerial bomb's position in the earth coordinate system (ECS) is $[x(t), y(t), z(t)]^T$, and its relative velocity vector $\boldsymbol{u}$ w.r.t. ECS is $[u_x(t), u_y(t), u_z(t)]^T$. We have

$$\begin{aligned}
\dot{u}_x &= f_1[\boldsymbol{X}(t), C_{df}(M)] = -\rho s V(u_x - w_x)C_{df}(M)/2m \\
\dot{u}_y &= f_2[\boldsymbol{X}(t), C_{df}(M)] = -\rho s V u_y C_{df}(M)/2m - g \\
\dot{u}_z &= f_3[\boldsymbol{X}(t), C_{df}(M)] = -\rho s V(u_z - w_z)C_{df}(M)/2m \\
\dot{x} &= f_4[\boldsymbol{X}(t), C_{df}(M)] = u_x \\
\dot{y} &= f_5[\boldsymbol{X}(t), C_{df}(M)] = u_y \\
\dot{z} &= f_6[\boldsymbol{X}(t), C_{df}(M)] = u_z
\end{aligned} \tag{1}$$

where $\boldsymbol{X}(t) = [x, y, z, u_x, u_y, u_z]^T$, which is the state vector of system (1); g is the gravitational acceleration; w_x, w_z are wind components in ECS; V is the aerial bomb's relative velocity w.r.t. wind and given by

$$V = \sqrt{(u_x - w_x)^2 + u_y^2 + (u_z - w_z)^2} \tag{2}$$

ρ is the air density; $s = \pi d^2/4$, which is the reference area of aerial bomb; d is the aerial bomb's diameter; and m is the mass of the aerial bomb. $C_{df}(M)$ is the fitting drag coefficient curve w.r.t. the trajectory model (1), which is regarded as a control profile to be solved. M denotes the Mach number and is given

Received Sept. 9, 1997; revision received April 17, 1998; accepted for publication July 5, 1998.

*Professional Officer, Department of Electrical Engineering, 10 Kent Ridge Crescent. E-mail: yqchen@shuya.ml.org.

†Senior Lecturer, School of Electrical and Electronic Engineering, Nanyang Avenue, E-mail: ecywen@ntu.edu.sg.

‡Associate Professor, Department of Electrical Engineering.

§Schwartz, A. L., E. Polak, and Y. Chen. "RIOTS_95 (Recursive Integration Optimal Trajectory Solver)—A Matlab Toolbox for Solving Optimal Control Problems," Version 1.0 for Windows. URL: http://turnpike.net/~RIOTS, 1997.

as $M = V/a$, where a is the local sonic speed. Denote $x_m(t)$, $y_m(t)$, $z_m(t)$ as measured trajectories from theodolite films. Let the functional index be

$$J[C_{df}(M)] = \int_{t_0}^{t_f} L[C_{df}(M), \boldsymbol{X}(t), t]\,\mathrm{d}t \tag{3}$$

where $L[C_{df}(M), \boldsymbol{X}(t), t] = [x(t) - x_m(t)]^2 + [y(t) - y_m(t)]^2 + [z(t) - z_m(t)]^2$. With t_0, t_f, and $\boldsymbol{X}_0$ given, C_{df} and $\boldsymbol{X}(t)$ are unconstrained, and with a free terminal condition, it is clear that Eqs. (1), (2), and (3) formulate an OTCP. It should be pointed out that this OTCP is a singular optimal control problem (SOCP), because of the form of Eq. (1), and the fact that L in Eq. (3) does not explicitly contain the time t and the control $C_{df}(M)$. Difficulties will arise in numerical computations for this SOCP. Furthermore, it is $C_{df}(M)$ instead of $C_{df}(t)$ that is to be extracted.

Optimal Dynamic Fitting

From the basic idea of the *optimal dynamic fitting* method, the first thing to do is to parameterize the control profile. Then an efficient parameter minimization method is to be employed. In this work, the control profile is parameterized by the cubic splines with a deficiency number of 2 and the parametric searching method is by the Newton–Raphson iteration.

Parameterization of $C_{df}(M)$

Suppose that $M \in (M_0, M_f)$, and (M_0, M_f) is divided into n segments with $n + 1$ kn $M_1(=M_0) < M_2 < \cdots < M_n < M_{n+1}(=M_f)$. (M_0, M_f) can be estimated to cover the practical Mach range. Denote f_i, d_i as the function value and the first-order derivative of $C_{df}(M)$ at the ith knot M_i, respectively. Consider the interval (M_i, M_{i+1}) and suppose $M \in (M_i, M_{i+1})$. Then a Hermite-type polynomial $C_{df_i}(M)$ can be uniquely determined by f_i, d_i, f_{i+1}, d_{i+1}. The cubic polynomial $C_{df_i}(M)$ can be expressed in the following forms:

$$\begin{aligned} C_{df_i}(M) &= [\gamma_1(\tau_i), \gamma_2(\tau_i), \gamma_3(\tau_i), \gamma_4(\tau_i)][f_i, d_i, f_{i+1}, d_{i+1}]^T \\ &= [\alpha_{1i}, \alpha_{2i}, \alpha_{3i}, \alpha_{4i}][1, M_i, M_i^2, M_i^3]^T \\ &= [\beta_{1i}, \beta_{2i}, \beta_{3i}, \beta_{4i}][1, \tau_i, \tau_i^2, \tau_i^3]^T \end{aligned} \tag{4}$$

where $\tau_i = (M - M_i)/h_i$, $h_i = M_{i+1} - M_i$. Obviously, $\tau_i \in [0, 1]$. The coefficients α, β, and γ in Eq. (4) are functions of t_i, h_i, and M_i. The detailed formulas can be found in Ref. 6. Now denote $\boldsymbol{C}^T = [c_1, c_2, \cdots, c_{2n+2}]$, where $c_{2i-1} = f_i$, $c_{2i} = d_i$ ($i = 1, 2, \cdots, n + 1$). Then the functional minimization problem $\min_{C_{df}} J[C_{df}]$ can be converted into a multivariable parametric minimization problem $\min_C J[C_{df}]$. A class of direct search methods can be used to solve this problem. But it will be less efficient when the dimension of $\boldsymbol{C}^T$ is large. In this case, the Newton–Raphson iteration is preferred. The problem is just turned to determine $\partial J/\partial c_i$ and $\partial^2 J/\partial c_i \partial c_j (i, j = 1, 2, \cdots, 2n + 2)$.

Newton–Raphson Iteration

Denote the Hamiltonian function $H[C_{df}, X(t), t]$ as

$$H = L + \boldsymbol{\lambda}^T \boldsymbol{f} \tag{5}$$

where $\boldsymbol{f} = [f_1, f_2, \cdots, f_6]^T$; $\boldsymbol{f}$ and L are defined in Eqs. (1) and (3), respectively; $\boldsymbol{\lambda} = [\lambda_1, \lambda_2, \cdots, \lambda_6]^T$ is the costate vector and

$$\frac{\mathrm{d}\boldsymbol{\lambda}}{\mathrm{d}t} = -\frac{\partial H}{\partial \boldsymbol{X}} = -\frac{\partial L}{\partial \boldsymbol{X}} - \boldsymbol{\lambda}^T \frac{\partial f}{\partial \boldsymbol{X}}, \qquad [\lambda(t_f) = 0] \tag{6}$$

A necessary optimality condition is that

$$\frac{\partial H}{\partial C_{df}} = \frac{\partial L}{\partial C_{df}} + \frac{\partial \boldsymbol{\lambda}^T \boldsymbol{f}}{\partial C_{df}} = 0 \tag{7}$$

From Eq. (7), we have $\partial L/\partial C_{df} = -\partial \boldsymbol{\lambda}^T \boldsymbol{f}/\partial C_{df}$. This implies that

$$\frac{\partial L}{\partial c_i} = -\frac{\partial \boldsymbol{\lambda}^T \boldsymbol{f}}{\partial C_{df}} \frac{\partial C_{df}}{\partial c_i} \tag{8}$$

So, integrating Eq. (8) from t_0 to t_f w.r.t. time t and denoting $\varsigma_i = \partial J/\partial c_i$, we have

$$\begin{aligned} \varsigma_i &= -\int_{t_0}^{t_f} \frac{\partial \boldsymbol{\lambda}^T \boldsymbol{f}}{\partial C_{df}} \frac{\partial C_{df}}{\partial c_i}\mathrm{d}t \\ &= -\int_{t_0}^{t_f} \frac{\rho s V}{2m}[\lambda_1(u_x - w_x) + \lambda_2 u_y + \lambda_3(u_z - w_z)] \frac{\partial C_{df}}{\partial c_i}\mathrm{d}t \end{aligned} \tag{9}$$

Then, by neglecting $\partial\rho/\partial c_j$, we can obtain

$$\begin{aligned} \frac{\partial \varsigma_i}{\partial c_j} = \frac{\partial^2 J}{\partial c_i \partial c_j} = -\int_{t_0}^{t_f} \frac{\rho s V}{2m} \Bigg[&\left(\frac{\partial V}{\partial c_j}\lambda_1 + V\frac{\partial \lambda_1}{\partial c_j}\right)(u_x - w_x) \\ &+ \left(\frac{\partial V}{\partial c_j}\lambda_2 + V\frac{\partial \lambda_2}{\partial c_j}\right)u_y + \left(\frac{\partial V}{\partial c_j}\lambda_3 + V\frac{\partial \lambda_3}{\partial c_j}\right)(u_z - w_z) \\ &+ \lambda_1\frac{\partial u_x}{\partial c_j} + \lambda_2\frac{\partial u_y}{\partial c_j} + \lambda_3\frac{\partial u_z}{\partial c_j}\Bigg]\frac{\partial C_{df}}{\partial c_i}\mathrm{d}t \end{aligned} \tag{10}$$

where $i, j = 1, 2, \cdots, 2n + 2$. Differentiating Eq. (1) w.r.t. c_j ($j = 1, 2, \cdots, 2n + 2$) gives

$$\frac{\mathrm{d}}{\mathrm{d}t}\left(\frac{\partial \boldsymbol{X}}{\partial c_j}\right) = \frac{\partial \boldsymbol{f}}{\partial c_j}, \qquad \left(\frac{\partial \boldsymbol{X}}{\partial c_j}\right)\bigg|_{t=t_0} = 0 \tag{11}$$

Similarly, by differentiating Eq. (6) w.r.t. $c_j (j = 1, 2, \cdots, 2n + 2)$, $\partial\boldsymbol{\lambda}/\partial c_j$ can be obtained

$$\frac{\mathrm{d}}{\mathrm{d}t}\left(\frac{\partial \boldsymbol{\lambda}}{\partial c_j}\right) = \frac{\partial H}{\partial \boldsymbol{X}}, \qquad \frac{\partial \boldsymbol{\lambda}}{\partial c_j}\bigg|_{t=t_f} = 0 \tag{12}$$

Integrating Eqs. (1) and (11) simultaneously from t_0 to t_f, then integrating Eqs. (6) and (12) simultaneously from t_f to t_0, ς_i and $\partial\varsigma_i/\partial c_i$ in Eqs. (9) and (10) can be computed by a proper quadrature algorithm. Thus, the Newton–Raphson iteration can be applied

$$\boldsymbol{C}^{(k+1)} = \boldsymbol{C}^{(k)} + \delta\boldsymbol{C}^{(k)} \tag{13}$$

$$\boldsymbol{A}^{(k)}\delta\boldsymbol{C}^{(k)} = \boldsymbol{B}^{(k)} \tag{14}$$

where k is the iteration number; $\delta\boldsymbol{C}^{(k)}$ is the optimal increment of $\boldsymbol{C}^{(k)}$ at the kth iteration. $\boldsymbol{A}^{(k)}$ and $\boldsymbol{B}^{(k)}$ are appropriate dimensional matrix and vector with elements $a_{i,j}$ and b_i, respectively. We know that

$$a_{i,j} = \frac{\partial \varsigma_i}{\partial c_i}, \qquad b_i = -\varsigma_i, \qquad i, j = 1, 2, \cdots, 2n + 2 \tag{15}$$

Attention must now be paid to the calculation of $\partial C_{df}/\partial c_i$. From Eq. (4), we get

$$\frac{\partial C_{df}}{\partial c_i} = \begin{cases} 0, & M \notin [M_k, M_{k+1}], \quad \forall\ i \\ \gamma_1(\tau_k), & M \in [M_k, M_{k+1}], \quad i \text{ is odd} \\ \gamma_2(\tau_k), & M \in [M_k, M_{k+1}], \quad i \text{ is even} \end{cases} \tag{16}$$

where $k = \mathrm{int}\{(i + 1)/2\}$, and $\mathrm{int}\{\cdot\}$ is an integer truncating operation. Furthermore, we know that the $M(t)$ curve is usually a U type, and that the minimal Mach number point corresponds to a trajectory apogee. Thus, we must consider the ascending trajectory and descending trajectory separately in the processes of forward and backward integration because $C_{df}(M)$ is param-

eterized w.r.t. M. Suppose that $M \in [M_k, M_{k+1}]$. If the current Mach number M is at the descending part of the trajectory, we know from the causality relations that in the forward integration of Eqs. (1) and (10)

$$\frac{\mathrm{d}}{\mathrm{d}t}\left(\frac{\partial \boldsymbol{X}}{\partial c_i}\right) = 0, \qquad i = 2k + 3, 2k + 4, \cdots, 2n + 2 \tag{17}$$

while in the backward integration of Eqs. (6) and (11)

$$\frac{\mathrm{d}}{\mathrm{d}t}\left(\frac{\partial \boldsymbol{\lambda}}{\partial c_i}\right) = 0, \qquad i = 1, 2, \cdots, 2k - 2 \tag{18}$$

Similarly, if the current Mach number M belongs to the ascending trajectory, we must set

$$\frac{\mathrm{d}}{\mathrm{d}t}\left(\frac{\partial \boldsymbol{X}}{\partial c_i}\right) = 0, \qquad i = 1, 2, \cdots, 2k - 2 \tag{19}$$

in the forward integration of Eqs. (1) and (10), and set

$$\frac{\mathrm{d}}{\mathrm{d}t}\left(\frac{\partial \boldsymbol{\lambda}}{\partial c_i}\right) = 0, \qquad i = 2k + 3, 2k + 4, \cdots, 2n + 2 \tag{20}$$

in the backward integration of Eqs. (6) and (11).

Quasi-Newton–Raphson Iteration

Total $12n + 18$ differential equations are to be integrated in a forward or backward direction. With a larger n, the computation in forward or backward integration is burdensome. To avoid the backward pass, simply taking the partial derivative w.r.t. c_i directly in Eq. (3) gives

$$\mathrm{s}_i = \frac{\partial J}{\partial c_i} = 2\int_{t_0}^{t_f}\left[(x - x_m)\frac{\partial x}{\partial c_i} + (y - y_m)\frac{\partial y}{\partial c_i} + (z - z_m)\frac{\partial z}{\partial c_i}\right]\mathrm{d}t \tag{21}$$

From Eq. (21), with abuse of notions, let

$$\frac{\partial \mathrm{s}_i}{\partial c_j} = 2\int_{t_0}^{t_f}\left(\frac{\partial x}{\partial c_i}\frac{\partial x}{\partial c_j} + \frac{\partial y}{\partial c_i}\frac{\partial y}{\partial c_j} + \frac{\partial z}{\partial c_i}\frac{\partial z}{\partial c_j}\right)\mathrm{d}t \tag{22}$$

Replacing Eqs. (9) and (10) with (21) and (22), respectively, forms the quasi-Newton–Raphson iterative scheme. This treatment was called *differential correction*.[1] In Eq. (22), terms related to the second-order partial derivatives $(x - x_m)\partial^2 x/\partial c_i \partial c_j$, $(y - y_m)\partial^2 y/\partial c_i \partial c_j$ and $(z - z_m)\partial^2 z/\partial c_i \partial c_j$ are neglected. With a properly chosen initial $\boldsymbol{C}^{(0)}$, which makes the iteration converge, the effect of the neglected terms will be increasingly smaller and the iteration approaches to a second-order convergence will be by using the first-order gradient alone.

Estimation of Inaccurate $X(0)$

When the initial condition $X(0)$ of Eq. (1) is unknown, we need to estimate it. In this case, its estimate $\hat{\boldsymbol{X}}(0)$ will be considered as a set of design parameters in the optimization procedure. This can be easily achieved in the optimal dynamic fitting method presented earlier. In this Note, the initial estimate of $\boldsymbol{X}(0)$ can be obtained from the measured data and the testing setup. To apply the quasi-Newton–Raphson method, the procedure for optimizing $\hat{\boldsymbol{X}}(0)$ is similar to that of $\boldsymbol{C}^T$. Referring to Eq. (11), 36 differential equations related to $\hat{\boldsymbol{X}}(0)$ can be determined similarly. The relevant initial integration conditions must be set to 0, except the following:

$$\begin{aligned} &\frac{\partial x}{\partial \hat{x}_0|_{t=t_0}} = 1, \quad \frac{\partial y}{\partial \hat{y}_0|_{t=t_0}} = 1, \quad \frac{\partial z}{\partial \hat{z}_0|_{t=t_0}} = 1 \\ &\frac{\partial u_x}{\partial u_{\hat{x}_0}|_{t=t_0}} = 1, \quad \frac{\partial u_y}{\partial u_{\hat{y}_0}|_{t=t_0}} = 1, \quad \frac{\partial u_z}{\partial u_{\hat{z}_0}|_{t=t_0}} = 1 \end{aligned} \tag{23}$$

where $\partial C_{df}/\partial \hat{\boldsymbol{X}}(0)$ is neglected.

Practical Results from Flight Tests

The main purpose of the flight tests is to finally measure $C_{df}(M)$ of the aerial bomb. Several tests were carried out under different bombing conditions. The collected data from flight paths No. 7, 8, and 9 are shown in Fig. 1, which were converted from the three-dimensional theodolite film data provided by a proving ground. According to the standardization processing result from the proving ground, for flight Nos. 7–9, respectively, the elevation angles when bombing are 0.15, 0.11, and −0.04 deg; the heights when bombing are 4101, 4103, and 4106 m, the velocities (m/s) when bombing are 127, 129, and 125; the obtained ballistic coefficients c are 0.60553,

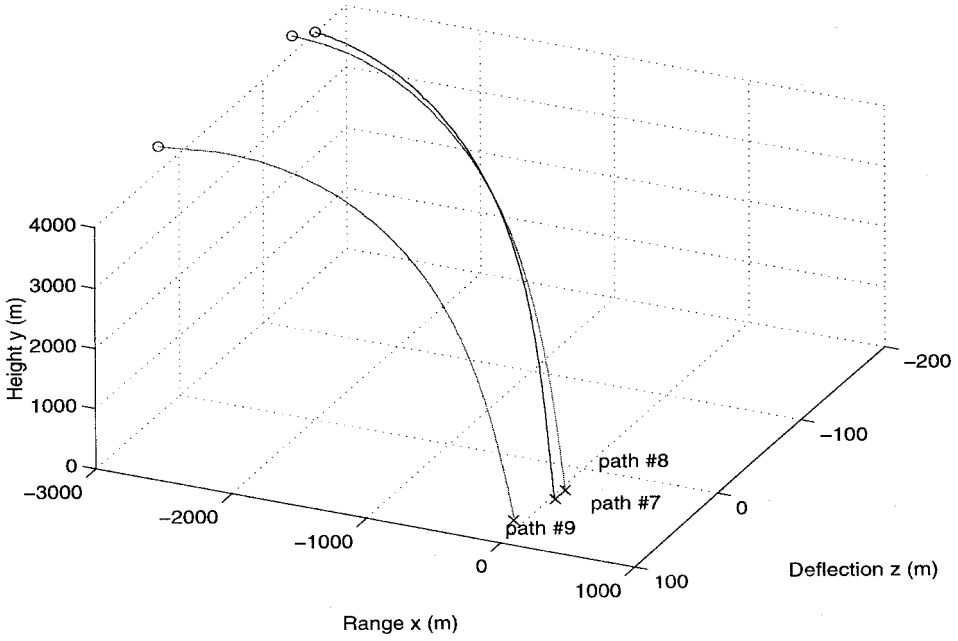

Fig. 1 Measured flight paths nos. 7, 8, and 9.

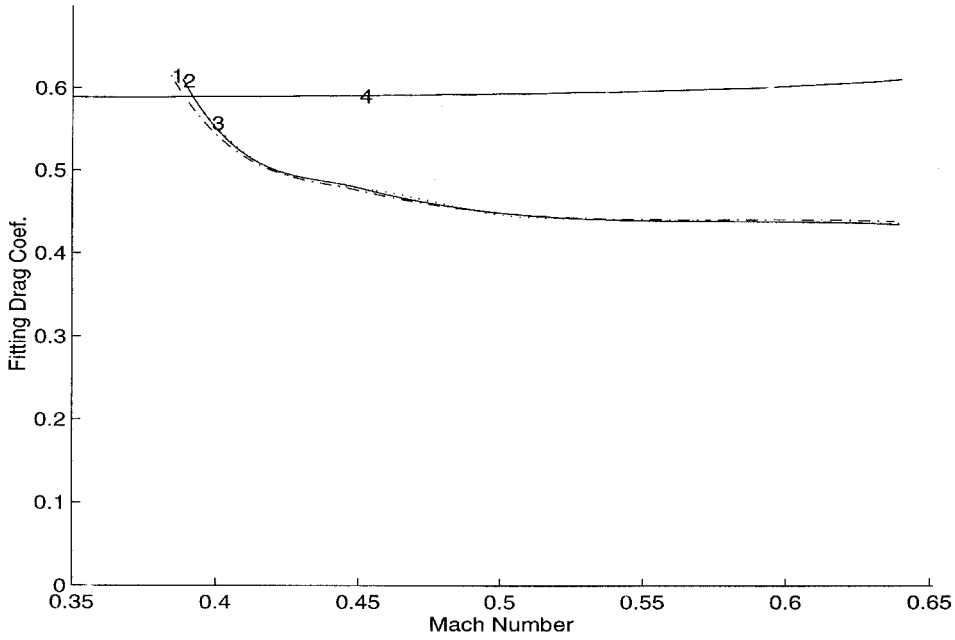

Fig. 2 $C_{df}(M)$ **by optimal dynamic fitting method from three flight paths' data.**

Table 1 Comparison of shape coefficients

Flight path no.	i_{cp1}	i_{cp2}	Shape coefficient error $(i_{cp1} - i_{cp2})/i_{cp1}$, %	Range error $\Delta A/A$, %
7	0.757	0.792	−4.616	−0.692
8	0.765	0.793	−3.639	−0.546
9	0.753	0.792	−5.167	−0.775
Average value	0.758	0.792	−4.474	−0.671

0.61213, and 0.60274; the obtained shape coefficients i_{cp1} are 0.757, 0.765, and 0.753. In the preceding text, c is obtained as a fitting factor to fit the range measurements under practical bombing conditions, i.e.,

$$c = id^2/m \times 10^3, \qquad i = c_x/\bar{c}_{x0} \tag{24}$$

where i is the aerial bomb's shape coefficient, c_x is the drag coefficient, and $\bar{c}_{x0}$ is the so-called drag-law. i_{cp1} is also a fitting result provided by the proving ground based on a fitted c.

Using the method and relevant data reduction program of this work, three $C_{df}(M)$ curves marked 1, 2, and 3, corresponding to flight path nos. 7, 8, and 9, respectively, are obtained (Fig. 2) where the curve marked with 4 is the drag-law $\bar{c}_{x0}(M)$ (local). From the results in Fig. 2, the shape coefficient curve $i(M)$ of each flight path can be determined

$$i(M) = C_{df}(M)/\bar{c}_{x0}(M) \tag{25}$$

Taking the mean value of this $i(M)$, we can get an average shape coefficient i_{cp2}. It is important to point out that i_{cp2} is with the comparability w.r.t. i_{cp1} provided by the proving ground. See Table 1 for the shape coefficient comparison and the induced relative range error $\Delta A/A$ comparison according to the evaluation formula of the proving ground. From Fig. 2 and Table 1, it can be concluded that the $C_{df}(M)$ curve identified is correct. The curve form of $C_{df}(M)$ fits to the qualitative theoretical understanding. In these sets of flight testing data, the maximal Mach number is about 0.65. Theoretically, $C_{df}(M)$ should be constant when $M \leq 0.65$ (lower subsonic region). But because of the interference airflow between the aircraft and the aerial bomb when bombing and the relevant induced angular motion around the c.m. of the aerial bomb, the shape of $C_{df}(M)$ is reasonable. It is interesting to note that $C_{df}(M)$ approximately exponentially decays in the earlier stage of Mach range and then smoothly transits to a constant value. The latter phenomenon fits to the aerodynamic theory as effects of interference flowfield to aerial bomb's motion have died out and the aerial bomb is almost in a free air flowfield.

Conclusions

The aerodynamic curve identification of aerial bomb from three-degree-of-freedom positional measurements is formulated as an OTCP. By using a spine parameterization of the drag coefficient curve that is taken as the control profile (Mach history), the OTCP is converted into a parametric minimization problem where the proposed quasi-Newton–Raphson iteration can be used to cut the computational cost by half compared with the standard Newton–Raphson iteration. The inaccurate initial states can also be corrected easily. The equivalence between the interference flowfield and the free flowfield could be studied based on the result of this Note. Furthermore, the method of this Note provides an effective way for solving a wider class of singular optimal control problems.

Acknowledgment

M. Sun was supported by the National Science Foundation of China under Project 69404004.

References

[1]Chapman, G. T., and Kirk, D. B., "A Method for Extracting Aerodynamic Coefficients from Free Flight Data," *AIAA Journal*, Vol. 8, No. 4, 1970, pp. 753–758.

[2]Fratter, C., and Stengel, R. F., "Identification of Aerodynamic Coefficients Using Flight Testing Data," AIAA Paper 83-2099, 1983.

[3]Larimore, W. E., Lebow, W. M., and Mehra, R. K., "Identification of Parameters and Model Structure for Missile Aerodynamics," *Proceedings of the American Control Conference* (Boston, MA), American Automatic Control Council, Evanston, IL, 1985, pp. 18–26.

[4]Anderson, L. C., and Vincent, J. H., "Application of System Identification to Aircraft Flight Test Data," *Proceedings of the 24th IEEE Conference on Decision and Control* (Fort Lauderdale, FL), Institute

of Electrical and Electronics Engineers, New York, 1985, pp. 1929–1931.

[5]Linse, D. J., and Stengel, R. F., "Identification of Aerodynamic Coefficients Using Computational Neural Networks," *Journal of Guidance, Control, and Dynamics*, Vol. 16, No. 6, 1994, pp. 1018–1025.

[6]Chen, Y., Wen, C., Gong, Z., and Sun, M., "Projectile's Aerodynamic Drag Coefficient Curve Identification from Radar Measured Velocity Data: Optimal Dynamic Fitting Approach," *Journal of Control Engineering Practice*, Vol. 5, No. 5, 1997, pp. 627–636.

Arbitrary Accuracy Integration Scheme for the Subsonic Doublet Lattice Method

Louw H. van Zyl*
Aerotek, CSIR, Pretoria 0001, South Africa

Nomenclature

D_1, D_2 = planar and nonplanar parts of the incremental oscillatory downwash factor
e = box semispan
k_r = reduced frequency based on box semichord or mean wing semichord
M = Mach number
$P^n(x)$ = polynomial of degree n in x
Δx = box chord
y, z = coordinates of collocation point in sending panel coordinate system
η = spanwise coordinate of sending point

Introduction

THE subsonic doublet lattice method,[1,2] used in the calculation of unsteady air loads on an aircraft, can be regarded as an extension of the vortex lattice method, which is used for steady load calculation. The downwash factors are calculated as the sum of the steady component, identical to that of the vortex lattice method, and an unsteady component. Whereas the steady component is exact, the unsteady component is approximated. The approximation in the unsteady component places a restriction on the doublet lattice method in terms of box aspect ratio, which does not apply to the vortex lattice method. The incremental oscillatory downwash factor is divided into a planar and a nonplanar part.[2] Each part is expressed as an integral over the length of the doublet line, of which the integrand is the planar or nonplanar kernel numerator divided by the square or fourth power, respectively, of the radial distance between the sending and receiving points. These integrals cannot be evaluated analytically, and the usual way of evaluating them is to make polynomial approximations to the numerators of the integrands and integrating the resulting expressions analytically. To obtain accurate results, the box aspect ratio must be limited. Reference 2, which describes the use of parabolic approximations, suggests using box aspect ratios not much greater than unity, whereas Ref. 3 suggests using box aspect ratios of less than three, also for a parabolic approximation.

Rodden et al.[4,5] described quartic approximations to the kernel numerators and suggested that the higher degree approximation may allow the use of aspect ratios of up to 10. To quantify the integration error in these production methods, it would be useful to have available a method that will converge to the correct result in an orderly manner as computational effort is increased. Increasing the degree of the approximating polynomials does not have the desired effect. The excursions between matched points get larger and the results diverge. The approach presented here is to make a natural cubic spline approximation to the kernel numerators, followed by analytical integration over each interval. General integration formulas, necessitated by the nonsymmetric integration intervals, are given. Results are presented that indicate that the method converges without difficulty.

Received March 1, 1998; revision received July 2, 1998; accepted for publication July 8, 1998.

*Engineer, Aeroelasticity Facility, P.O. Box 395. E-mail: lvzyl@csir.co.za.

General Integration Formulas

The incremental (unsteady) downwash factor is divided into a planar and a nonplanar part as was done in Ref. 2, but polynomials of arbitrary degree are substituted for the parabolas

$$D_1 = \frac{\Delta x}{8\pi}\int_{\eta_1}^{\eta_2} \frac{P_1^n(\eta)}{(y-\eta)^2 + z^2}\,d\eta \tag{1}$$

$$D_2 = \frac{\Delta x}{8\pi}\int_{\eta_1}^{\eta_2} \frac{P_2^n(\eta)}{[(y-\eta)^2 + z^2]^2}\,d\eta \tag{2}$$

The numerators are divided by the denominators to obtain

$$D_1 = \frac{\Delta x}{8\pi}\int_{\eta_1}^{\eta_2} \left[P^{n-2}(\eta) + \frac{a_1\eta + a_0}{(y-\eta)^2 + z^2}\right]d\eta \tag{3}$$

$$D_2 = \frac{\Delta x}{8\pi}\int_{\eta_1}^{\eta_2} \left[P^{n-4}(\eta) + \frac{b_3\eta^3 + b_2\eta^2 + b_1\eta + b_0}{[(y-\eta)^2 + z^2]^2}\right]d\eta \tag{4}$$

The polynomials are simple to integrate, whereas the method of partial fractions can be used to integrate the fractions. The fraction in the nonplanar integrand is expressed in terms of its partial fractions as

$$\frac{a+ib}{\eta-(y+iz)} + \frac{a-ib}{\eta-(y-iz)} + \frac{c+id}{[\eta-(y+iz)]^2} + \frac{c-id}{[\eta-(y-iz)]^2} \tag{5}$$

where

$$a = b_3/2 \tag{6}$$

$$b = -[b_0 + yb_1 + (y^2+z^2)b_2 + y(y^2+3z^2)b_3]/4z^3 \tag{7}$$

$$c = -[b_0 + yb_1 + (y^2-z^2)b_2 + y(y^2-3z^2)b_3]/4z^2 \tag{8}$$

$$d = -[b_1 + 2yb_2 + (3y^2-z^2)b_3]/4z \tag{9}$$

The first two partial fractions integrate to logarithmic functions, whereas the last two integrate to simple reciprocals. If $z = 0$, the result for the planar part is given by

$$D_1 = P^{n-1}(\eta_2) - P^{n-1}(\eta_1) + a_1\,\ell n\left|\frac{y-\eta_2}{y-\eta_1}\right| + (a_1y + a_0)\left(\frac{1}{y-\eta_2} - \frac{1}{y-\eta_1}\right) \tag{10}$$

If $z \neq 0$, the planar and nonplanar parts are given by

$$D_1 = P^{n-1}(\eta_2) - P^{n-1}(\eta_1) + \frac{a_1}{2}\,\ell n\frac{(y-\eta_2)^2+z^2}{(y-\eta_1)^2+z^2} + \frac{a_1y + a_0}{2z}\arg[f + iz(\eta_2 - \eta_1)] \tag{11}$$